Sturtevant, J. (1977) *Proc. Natl. Acad. Sci. U.S.A. 74*, 2236–2240.
Tittor, J., Soell, C., Oesterhelt, D., Butt, H.-J., & Bamberg, E. (1989) *EMBO J. 8*, 3477–3482.
Vârô, G., & Lanyi, J. K. (1990) *Biochemistry 29*, 2241–2250.
Vârô, G., & Lanyi, J. K. (1991a) *Biochemistry 30*, 5008–5015.
Vârô, G., & Lanyi, J. K. (1991b) *Biochemistry 30*, 5016–5022.
Vârô, G., & Lanyi, J. K. (1991c) *Biophys. J. 59*, 313–322.
Vârô, G., Duschl, A., & Lanyi, J. K. (1990) *Biochemistry 29*, 3798–3804.
Walmsley, A. R., & Lowe, A. G. (1987) *Biochim. Biophys. Acta 901*, 2229–2238.
Zimányi, L., Keszthelyi, L., & Lanyi, J. K. (1989) *Biochemistry 28*, 5165–5172.

Effects of Melittin on Molecular Dynamics and Ca-ATPase Activity in Sarcoplasmic Reticulum Membranes: Electron Paramagnetic Resonance†

James E. Mahaney and David D. Thomas*
Department of Biochemistry, University of Minnesota Medical School, Minneapolis, Minnesota 55455
Received February 11, 1991; Revised Manuscript Received May 10, 1991

ABSTRACT: We have performed electron paramagnetic resonance (EPR) experiments on nitroxide spin labels incorporated into rabbit skeletal sarcoplasmic reticulum (SR), in order to investigate the physical and functional interactions between melittin, a small basic membrane-binding peptide, and the Ca-ATPase of SR. Melittin binding to SR substantially inhibits Ca^{2+}-dependent ATPase activity at 25 °C, with half-maximal inhibition at 9 mol of melittin bound per mole of Ca-ATPase. Saturation transfer EPR (ST-EPR) of maleimide spin-labeled Ca-ATPase showed that melittin decreases the submillisecond rotational mobility of the enzyme, with a 4-fold increase in the effective rotational correlation time (τ_r) at a melittin/Ca-ATPase mole ratio of 10:1. This decreased rotational motion is consistent with melittin-induced aggregation of the Ca-ATPase. Conventional EPR was used to measure the submicrosecond rotational dynamics of spin-labeled stearic acid probes incorporated into SR. Melittin binding to SR at a melittin/Ca-ATPase mole ratio of 10:1 decreases lipid hydrocarbon chain mobility (fluidity) 25% near the surface of the membrane, but only 5% near the center of the bilayer. This gradient effect of melittin on SR fluidity suggests that melittin interacts primarily with the membrane surface. For all of these melittin effects (on enzymatic activity, protein mobility, and fluidity), increasing the ionic strength lessened the effect of melittin but did not alleviate it entirely. This is consistent with a melittin–SR interaction characterized by both hydrophobic and electrostatic forces. Since the effect of melittin on lipid fluidity alone is too small to account for the large inhibition of Ca-ATPase rotational mobility and enzymatic activity, we propose that melittin inhibits the ATPase primarily through its capacity to aggregate the enzyme, consistent with previous observations of decreased Ca-ATPase activity under conditions that decrease protein rotational mobility.

Understanding the relationship between molecular dynamics and enzymatic activity within a biological membrane is a vital step toward constructing an accurate model describing the overall functioning of the membrane system. Concerning skeletal muscle sarcoplasmic reticulum (SR)[1] membranes, intensive research effort has been devoted to such an understanding; that is, to understand precisely how the molecular motions and interactions of both the Ca-ATPase, the major integral membrane protein of SR, and the lipids within the SR membrane contribute to the optimal functioning of calcium uptake.

Since the rotational mobility (diffusion coefficient) of an integral membrane protein about the membrane normal depends inversely on both the protein's cross-sectional area and the lipid hydrocarbon chain viscosity (Saffman & Delbrück, 1975), a variety of mechanisms designed to alter the physical state of the protein and the bilayer have been employed in order to correlate these perturbations with resultant Ca-ATPase functioning. Inducing lateral aggregation of the enzyme by either (a) changing temperature (Bigelow et al., 1986; Squier et al., 1988b; Birmachu & Thomas, 1990), (b) selectively cross-linking the Ca-ATPase (Squier et al., 1988a), (c) decreasing the lipid/protein ratio (Squier & Thomas, 1988), or (d) crystallizing the ATPase by using vanadate (Lewis & Thomas, 1986) has a profound inhibitory effect on both ATP hydrolysis and calcium uptake by SR. Increasing the fluidity (decreasing the viscosity) of the SR lipids adjacent to the protein results in an increased rate of Ca-ATPase rotation and a concomitant increase in Ca-ATPase activity (Bigelow & Thomas, 1987). The results of these studies indicate that optimal Ca-ATPase enzymatic function correlates directly with the ability of the Ca-ATPase to undergo microsecond rotational motion in a fluid lipid bilayer. Similar studies of other membrane-enzyme systems show that changes in lipid chain unsaturation or levels of cholesterol (which alter the fluidity of the bilayer) can have profound effects on function (Benga

† This work was supported by NIH Grant GM27906 to D.D.T. J.E.M. was supported by a postdoctoral fellowship from the American Heart Association.
* Author to whom correspondence should be addressed.

[1] Abbreviations: SR, sarcoplasmic reticulum; NEM, *N*-ethylmaleimide; MSL, maleimide spin label; SASL, stearic acid spin label; PCSL, phosphatidylcholine spin label; MOPS, 3-(*N*-morpholino)propanesulfonic acid; ATP, adenosine triphosphate; EPR, electron spin resonance; ST-EPR, saturation transfer EPR; $\int V_2'$, ST-EPR integrated intensity parameter; TPX, tetramethylene polymer plastic.

0006-2960/91/0430-7171$02.50/0

& Holmes, 1984; Shinitzky, 1984; Yeagle, 1985).

There is a class of amphipathic membrane-binding basic peptides known to alter the physical state of proteins and/or lipids in membranes. Understanding the mechanism of action of these peptides is an interesting problem, primarily due to the peptides' unique ability to interact electrostatically with protein and lipid surface charges while interacting hydrophobically with the hydrocarbon phase of lipid bilayers. This is best illustrated by melittin, a 26-residue peptide isolated from honey bee venom [reviewed by Dempsey (1990)]. Melittin binds to a variety of proteins, such as calmodulin (Raynor et al., 1991; Kataoka et al., 1989; Malencik & Anderson, 1985), protein kinase C (Raynor et al., 1991; O'Brian & Ward, 1989), H^+,K^+-ATPase (Cuppoletti et al., 1990), and myosin light chains (Malencik & Anderson, 1988). Among the effects of binding to proteins, melittin has been shown to inhibit strongly the rotational motion of membrane proteins bacteriorhodopsin and erythrocyte band 3 by inducing protein aggregation, presumably via the electrostatic binding and cross-linking of these proteins by melittin (Clague & Cherry, 1988, 1989; Dufton et al., 1984a,b; Hu et al., 1985; Hui et al., 1990). Melittin also binds to model bilayers (Dempsey & Sternberg, 1991; Dempsey et al., 1989; Schwarz & Beschiaschvili, 1989; Schulze et al., 1987), inducing changes in lipid chain order and dynamics (Bradrick et al., 1987; Prendergast et al., 1982; Faucon & Lakowicz, 1987), phase transition behavior (Bradrick et al., 1989; Lafleur et al., 1989; Dufourc et al., 1986), and head-group conformation (Kuchinka & Seelig, 1989; Beschiaschvilli & Seelig, 1990). Structural analyses of melittin have shown that the success of the peptide in binding and perturbing membrane proteins and/or lipids lies both in its extreme amphipathic character and the high density of basic (positively charged) residues in its sequence, allowing the peptide to interact effectively with both surface anions (from protein or lipid) and lipid hydrocarbon chains.

In the present study, we use melittin to perturb (a) the rotational mobility of the Ca-ATPase and (b) the hydrocarbon chain dynamics in SR vesicles, while correlating these changes with effects on Ca-ATPase activity. Submillisecond protein rotational mobility was measured by saturation transfer EPR, and submicrosecond lipid chain motions were measured by conventional EPR. While melittin is not expected to target SR membranes in vivo, our detailed understanding of the relationship between SR molecular dynamics and Ca-ATPase activity makes SR an excellent model membrane for investigating the mechanism of action of membrane-binding peptides upon their target membranes. The results of this study, along with those of a complimentary optical spectroscopic study (Voss et al., 1991), provide new insight into the interaction of melittin with a functioning membrane system, and strengthen our understanding of how the molecular motions and interactions of the Ca-ATPase and its associated lipids contribute to the optimal functioning of calcium uptake by SR membranes.

Materials and Methods

Reagents and Solutions. All spin labels were obtained from Aldrich. ATP, MOPS, and melittin were obtained from Sigma. All other reagents were obtained from Mallinckrodt and were of the highest purity available. All enzymatic assays and EPR experiments were carried out at 25 °C in a buffer containing either 60 mM KCl, 6 mM $MgCl_2$, 0.1 mM $CaCl_2$, and 20 mM MOPS, pH 7.0 (henceforth denoted as normal ionic strength), or the same buffer containing 0.5 M LiCl (henceforth denoted as high ionic strength), unless otherwise stated.

Preparations and Assays. Sarcoplasmic reticulum (SR) vesicles were prepared from the fast twitch skeletal muscle of New Zealand white rabbits (Fernandez et al., 1980). The vesicles were purified on a discontinuous sucrose gradient (Birmachu et al., 1989) to remove heavy SR vesicles (junctional SR containing calcium release proteins). All preparation was done at 4 °C. SR pellets were resuspended in 0.3 M sucrose and 20 mM MOPS (pH 7.0), rapidly frozen, and stored in liquid nitrogen until use. SR vesicles prepared in this fashion were typically 80 ± 5% Ca-ATPase (i.e., 7.2 nmol of Ca-ATPase/mg of SR protein) and contained approximately 80 phospholipids/Ca-ATPase (i.e., 580 nmol of phospholipid/mg of SR protein) (Bigelow et al., 1986). The ATP hydrolysis of the SR vesicles was fully coupled to calcium transport (Squier & Thomas, 1989).

SR lipids were extracted by a modification (Hidalgo et al., 1976) of the method of Folch et al. (1957), with nitrogen-saturated solvents to prevent oxidation. The lipids were stored in chloroform/methanol (2:1) under nitrogen at −20 °C. Unilamellar vesicles of extracted SR lipids were prepared as follows. Lipids dissolved in chloroform/methanol (2:1) were dried under a stream of nitrogen, lyophilized for at least 3 h to remove any traces of organic solvent, and then were rehydrated in normal ionic strength buffer by pulsed and rapid vortexing. Any lipid residue remaining on the sample vial wall was loosened by gentle scraping, followed by additional vortexing. The final concentration of the rehydrated lipids was adjusted to 5 mg/mL. The solution was subjected to five freeze–thaw cycles and then passed ten times, under nitrogen pressure, through two 0.1-μm polycarbonate filters (Nucleopore) in an extrusion device. The resulting solution was concentrated 10-fold, under nitrogen pressure, in an Amicon stirred cell ultraconcentrator. The resulting liposomes were 0.1 μm as determined by light scattering. The final lipid vesicle suspension was diluted to 60 mM for EPR analysis and stored at 4 °C.

Calcium-dependent ATPase activity was measured as described by Squier and Thomas (1989). The molar concentration of phospholipids in SR and SR lipid extracts and samples was determined from phosphorous assays (Chen et al., 1956). SR protein concentrations were determined by the biuret assay (Gornall et al., 1949) using bovine serum albumin as a standard.

Melittin was purified according to Wille (1989), with modifications described by Voss et al. (1991). The purified melittin preparations used in this study contained no detectable phospholipase activity, as assayed by the procedure of Wille (1989). Stock solutions of melittin were prepared in the experimental buffer by using lyophilized melittin. The concentration of these stock solutions was determined from the absorbance at 280 nm using $\epsilon_{280} = 5400\ M^{-1}\ cm^{-1}$.

Spin Labeling and Sample Preparation. The overall rotational mobility of the Ca-ATPase was measured by using the short-chain maleimide spin label, *N*-(1-oxyl-2,2,6,6-tetramethyl-4-piperadinyl)maleimide (MSL; Figure 1), covalently bound to the ATPase (MSL-Ca-ATPase) as described by Bigelow et al. (1986), with the omission of the 37 °C incubation of the final membrane pellet. Spin labeling the enzyme by this method results in (a) 1.2 mol of spin label per 10^5 g of SR protein, (b) no loss of Ca-ATPase or Ca^{2+}-uptake activity, and (c) ST-EPR spectra that report directly the overall rotational mobility of the protein (Lewis & Thomas, 1986; Squier & Thomas, 1986b; Squier et al., 1988a).

Hydrocarbon chain rotational mobility was measured with stearic acid spin labels (designated N-SASL), which are

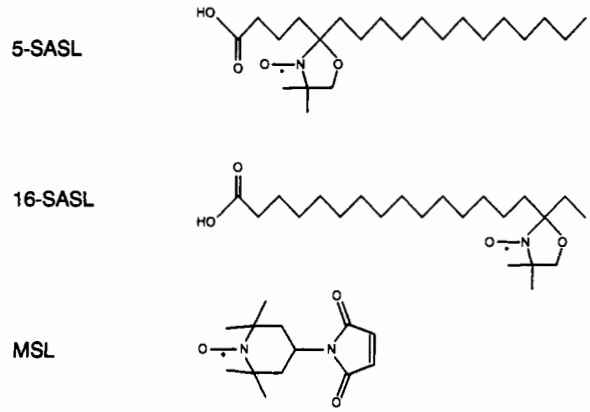

FIGURE 1: The spin labels used in this study. 5- and 16-SASL (stearic acid spin label), which are *N*-oxyl-4′,4′-dimethyloxazolidine derivatives of stearic acid spin label, were incorporated noncovalently into SR and SR lipid vesicles to monitor lipid hydrocarbon chain dynamics. MSL (4-maleimido-2,2,6,6-tetramethylpiperidinoxyl) was covalently bound to the Ca-ATPase to measure its microsecond rotational motions.

N-oxyl-4′,4′-dimethyloxazolidine derivatives of stearic acid. The labels used in the present study, 5- and 16-SASL, are shown in Figure 1. Prior to incorporation into SR, these labels were diluted from a dimethylformamide stock solution into ethanol (due to the greater miscibility of ethanol with water). A sufficient amount of label was added to SR (25 mg/mL in 0.3 M sucrose and 20 mM MOPS, pH 7.0, at 25 °C) to provide a ratio of 1 label per 200 phospholipids while keeping the final ethanol concentration in all samples below 1%. The labeled SR was vortexed well, diluted by a factor of 10 with experimental buffer, and pelleted in a low-speed table top centrifuge to remove any unbound label. For SASL incorporation into protein-free lipid vesicle samples, aliquots of the 0.1 M SASL stock solutions were used to prevent sample dilution and to keep the amount of organic solvent in the samples below 1%. The respective spin labels were added to the liposomes (1 label per 200 phospholipids) under vortex, followed by additional vortexing. SASL sample concentrations were kept sufficiently high (>50 mg/mL SR; >50 mM SR lipids) to minimize the spectral contribution from unbound aqueous labels. Labeling was carried out at 25 °C.

A similar derivative of phosphatidylcholine, 5-PCSL (not shown), was also used. The 5-PCSL was diluted from a DMF stock solution to 2 mg/mL in ethanol. The label was rapidly added to SR (3 mg/mL in 0.3 M sucrose and 20 mM MOPS, pH 7.0, at 25 °C) while vortexing, and the mixture was incubated for 30 min at 25 °C with intermittent vortexing. The SR was diluted into 0.3 M sucrose and 20 mM MOPS, pH 7.0, washed by centrifugation at 100000*g* for 50 min at 4 °C, and resuspended in the desired experimental buffer.

SR samples containing melittin were prepared by first diluting melittin from a stock solution (>10 mM melittin in normal ionic strength buffer) into experimental buffer followed by the addition of 2 mg of spin-labeled SR (final volume 1 mL). The melittin-containing SR was pelleted in a low-speed table top centrifuge to concentrate the membranes in preparation for EPR analysis. No-melittin control samples were treated identically, substituting buffer for melittin. All samples were prepared at 25 °C, and sample concentrations were 50 mg of SR/mL or higher. SR lipid samples containing melittin were prepared by adding melittin directly to the SR lipid vesicles under vortex, followed by additional vortexing. To preserve the integrity of the lipid bilayers in these studies, the amount of melittin added to the protein-free lipid samples was kept low (Dempsey & Sternberg, 1991; Dempsey, 1990); that is, at or below 5 mol of melittin per 80 mol of SR lipids (equivalent to the melittin/Ca-ATPase mole ratio of 5:1). None of the protein-free lipid spectra contained evidence of melittin-induced spectral heterogeneity, which would arise from the formation of melittin–lipid–probe micelles in our samples (Dempsey, 1990). All samples were prepared at 25 °C, and sample concentrations were 50 mM phospholipid or higher.

EPR Spectroscopy. EPR spectra were acquired with a Bruker ESP-300 spectrometer equipped with a Bruker ER4201 cavity, and digitized with the spectrometer's built-in microcomputer using Bruker OS-9-compatible ESP 1620 spectral acquisition software. Spectra were downloaded to an IBM-compatible microcomputer and analyzed with software developed in our laboratory by R. L. H. Bennett. Conventional (V_1) EPR was used to detect submicrosecond motions of both the lipid spin labels and the MSL–Ca-ATPase, and saturation transfer EPR (ST-EPR, V_2') was used to detect submillisecond motions of MSL–Ca-ATPase. V_1 spectra were obtained with 100-kHz field modulation (with a peak-to-peak modulation amplitude of 2 G), with microwave field intensities (H_1) of 0.032 G for MSL–Ca-ATPase and 0.14 G for SASL. V_2' spectra of the MSL–Ca-ATPase were obtained with 50-kHz field modulation (with a peak-to-peak modulation amplitude of 5 G), with a microwave field intensity of 0.25 G. Lipid spin label samples were contained in glass capillaries, whereas maleimide spin-labeled Ca-ATPase samples were contained in gas-permeable capillaries made of TPX (Popp & Hyde, 1981), allowing the removal of dissolved oxygen by purging the samples with N_2 (Squier & Thomas, 1986a). The sample temperature was controlled to within 0.5 °C with a Bruker ER 4111 variable temperature controller. The sample temperature was monitored with a Sensortek Bat-21 digital thermometer with an IT-21 thermocouple probe inserted into the top of the sample capillary, such that it did not interfere with spectral acquisition.

EPR Spectral Analysis. ST-EPR spectra of MSL-Ca-ATPase in SR were analyzed with the V_2' integrated intensity parameter (Squier & Thomas, 1986a). Effective rotational correlation times (τ_r) in SR were determined from a standard curve constructed from an isotropically tumbling model system (Squier & Thomas, 1986a). The protein rotational mobility, calculated as the inverse of the rotational correlation time, provides a parameter proportional to the rotational diffusion coefficient and lipid fluidity (Squier et al., 1988b; discussed below).

Fatty acid spin label spectra were analyzed by measuring the inner ($2T_\perp'$) and outer ($2T_\parallel'$) spectral splittings, sensitive mainly to the rotational amplitude, and the half-width at half-height of the low-field peak (Δ_L), sensitive mainly to the rate of motion. The effective order parameter (S) was calculated from the splittings in two essentially equivalent ways. First, spectra having well-resolved extrema (S greater than 0.3), so that both $2T_\parallel'$ and $2T_\perp'$ could be measured, were analyzed according to (Gaffney, 1976)

$$S = \frac{T_\parallel' - (T_\perp' - C)}{T_\parallel' + 2(T_\perp' + C)} \times 1.66 \qquad (1)$$

where $C = 1.4 - 0.053(T_\parallel' - T_\perp')$ and $2T_\parallel'$ and $2T_\perp'$ are the measured splittings between the inner and outer extrema resolved in the EPR spectrum (see Figure 4). For 16-SASL spectra, where S was always less than 0.3, eq 1 was not valid for calculating the effective order parameter (Squier et al., 1988). Therefore, 16-SASL order parameters were determined by the expression (Gaffney, 1976)

$$S = \frac{T_o - T_\perp'}{T_o - T_\perp} \quad (2)$$

where T_o is the isotropic hyperfine splitting constant in the absence of anisotropic effects, and $T_\perp$ is the minimum value of the effective hyperfine tensor for an axially symmetric system (e.g., a lipid bilayer). The values of T_o and $T_\perp$ used in this study were 14.3 ± 0.2 G and 6.3 ± 0.3 G, respectively, as previously determined by Squier and Thomas (1989).

To facilitate direct comparisons between melittin-induced changes in SR lipid hydrocarbon chain dynamics and protein rotational mobility, the effective lipid fluidity parameter T/η was used (Squier et al., 1988b):

$$S = -0.42\left(\log \frac{T}{\eta}\right) + 0.56 \quad (3)$$

where S is the apparent order parameter measured from the V_1 spectrum of either 5- or 16-SASL, and η is the effective lipid viscosity. This is consistent with conventional qualitative definitions of lipid fluidity, since (a) an increase in the fluidity (T/η) corresponds to a decrease in S, i.e., an increase in the amplitude of hydrocarbon chain reorientation, and (b) it yields a higher fluidity value (more motional freedom) near the center of the bilayer than near the head-group region (Squier et al., 1988b). However, eq 3 differs from conventional fluidity expressions, because (a) it is based on an empirical calibration in which EPR experiments were performed on solvents of known viscosity η, and (b) the resulting measurement of lipid fluidity (T/η) agrees quantitatively with the hydrodynamic theory of Saffman and Delbrück (1975), which predicts that the rotational mobility (diffusion coefficient D_m) of an integral membrane protein about the membrane normal should be proportional to T/η and inversely proportional to the area of the rotating unit (πa^2) in the plane of a membrane of thickness h:

$$D_m = kT/4\pi a^2 h\eta \quad (4)$$

Protein rotational correlation times, measured by ST-EPR and phosphorescence anisotropy, are inversely proportional to D_m (Thomas, 1986). The validity of this EPR-based fluidity measurement is supported by the finding that the rotational mobility (inverse correlation time) of the Ca-ATPase, as measured either by ST-EPR (Squier et al., 1988b) or phosphorescence anisotropy (Birmachu & Thomas, 1990), agrees quantitatively with the predictions of eq 4, as long as eq 3 is used to define T/η. Thus this fluidity parameter, along with eq 4, can be used to determine whether melittin-induced changes in Ca-ATPase rotational mobility are due to changes in lipid fluidity (T/η) or to changes in the size (aggregation state) of the rotating proteins.

Clearly, the fatty acid spin labels incorporated into SR are sampling a heterogeneous environment (Hidalgo, 1985; Bigelow & Thomas, 1987). A given spectrum arises from labels in a bulk lipid environment, labels in the restricted environment of the protein's lipid annular ring(s), labels affected by bound melittin, and labels in transition between these environments. Thus the effective values calculated for order parameters (S) and fluidities (T/η) are complex averages and do not represent rigorous measurements of actual lipid chain amplitudes, but they do provide a useful empirical tool for assessing changes in these parameters induced by melittin.

Results

Melittin Binding to SR Membranes and Ca-ATPase Inhibition. To ascertain the extent of melittin binding to SR, Voss et al. (1991) used a centrifugation binding assay to show

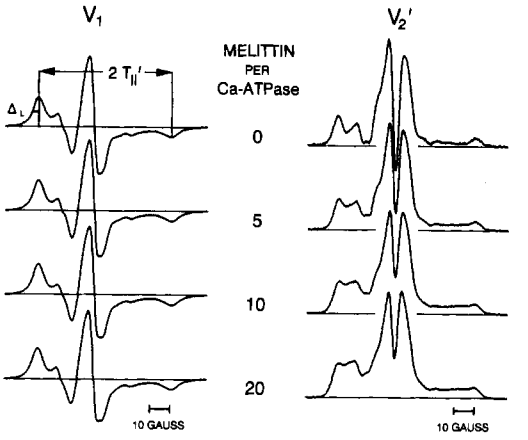

FIGURE 2: Effect of melittin on conventional (V_1) and saturation transfer EPR spectra of MSL–Ca-ATPase at 25 °C. Labeled SR was incubated with melittin at normal ionic strength for 30 min at 25 °C and prepared for EPR analysis as described under Materials and Methods. V_1 spectra (left) were virtually unchanged by the presence of melittin, as characterized by the outer splitting $2T_\parallel'$ and the half-width at half-height of the low-field peak Δ_L. Conversely, V_2' spectra (right) were quite sensitive to the presence of melittin, as characterized by increases in the total integrated intensity $\int V_2'$ of each spectrum with increasing melittin (Table I). Baselines represent 100 G.

that incubation of melittin with SR vesicles at mole ratios up to 20:1 (melittin/Ca-ATPase) results in essentially quantitative melittin binding to the membrane at normal ionic strength. At high ionic strength, melittin binding was reduced only slightly; i.e., most of the added melittin binds to SR even at high ionic strength. Further, Voss et al. (1991) have shown that melittin binding to SR membranes at normal ionic strength inhibits Ca-ATPase activity. The inhibition is biphasic, consisting of a steep 28% decrease in Ca-ATPase activity as melittin is added to SR up to a mole ratio of 3:1 (melittin/Ca-ATPase), followed by a more gradual inhibition at higher melittin/Ca-ATPase mole ratios. Nearly all activity is abolished at a ratio of 20:1. The addition of 0.5 M LiCl (high ionic strength) has virtually no effect on the steep early phase of inhibition (0–3 melittin per Ca-ATPase) but completely abolishes the second phase of inhibition (Voss et al., 1991). This suggests that the first phase may arise primarily from hydrophobic interactions between melittin and the membrane, with the second phase arising primarily from electrostatic interactions.

Effect of Melittin Binding on Ca-ATPase Rotational Motion. We used the maleimide spin label (MSL) covalently bound to the Ca-ATPase to observe the overall rotational motion of the enzyme by ST-EPR as a function of melittin binding to SR. Conventional EPR (V_1) and ST-EPR (V_2') spectra of the MSL–Ca-ATPase incubated with melittin are shown in Figure 2. Melittin binding to SR results in no change in the V_1 spectra, as shown by the virtually unchanging values of the outer splitting, $2T_\parallel'$ (67.0 ± 0.2 G) and half-width at half-height of the low-field peak, Δ_L (3.0 ± 0.1 G). In contrast, the V_2' spectra, which report the overall rotational motion of the MSL–Ca-ATPase (Lewis & Thomas, 1986; Squier et al., 1988a), are very sensitive to progressive melittin binding (Figure 2, Table I), determined by large increases in the total integrated intensity of the spectra, $\int V_2'$ (Squier & Thomas, 1986a). Figure 3 shows that the effective correlation time (τ_r), determined from $\int V_2'$ as described by Squier and Thomas (1986), increases steeply from 9 ± 3 μs (control) to 34 ± 11 μs at a melittin/Ca-ATPase mole ratio of 10:1 (3.7 times the control value), followed by a more gradual increase to 47 ± 25 μs at a ratio of 20:1 (5.2 times the control value).

Table I: Effect of Melittin on Ca-ATPase Rotational Mobility[a]

moles of melittin per mole of Ca-ATPase	$\int V_2' \times 10^3$	τ_r (μs)	normalized mobility
control	1.05 ± 0.12	9 ± 3	1.00
1:1	1.09 ± 0.13	11 ± 3	0.82
3:1	1.18 ± 0.15	18 ± 5	0.50
5:1	1.35 ± 0.16	24 ± 8	0.37
10:1	1.49 ± 0.12	34 ± 11	0.26
20:1	1.63 ± 0.15	47 ± 25	0.19

[a] MSL–Ca-ATPase mobility ($1/\tau_r$, μs^{-1}) was calculated from the effective rotational correlation time, τ_r, obtained from $\int V_2'$ as described under Materials and Methods. The mobility of each sample as a function of melittin ($1/\tau_{r,i}$) is shown normalized to the respective control no-melittin value ($1/\tau_{r,o}$) to allow a direct comparison between samples. Errors listed are standard deviations of at least three repetitions.

The increasing correlation times observed with increasing melittin indicate that melittin inhibits Ca-ATPase rotational motion. These effects are summarized in Table I. This effect of melittin on Ca-ATPase rotational motion is significantly reduced by high ionic strength (data not shown). At melittin/Ca-ATPase mole ratios of 5:1 and 10:1, the effective rotational correlation times are nearly 2-fold shorter than those obtained at normal ionic strength, showing that high ionic strength partially protects Ca-ATPase rotational mobility from inhibition by melittin. The effect of melittin is not completely eliminated at high ionic strength, supporting the proposal (above) that the interaction of melittin with SR is characteristic of both hydrophobic and electrostatic forces.

Effects of Melittin on Lipid Chain Dynamics in SR. The effects of melittin binding on the lipid hydrocarbon chain dynamics in SR were measured by using stearic acid spin labels (SASL, Figure 1). 5-SASL was used to measure melittin effects on chain dynamics near the head-group region of the bilayer and 16-SASL was used to measure melittin effects on chain dynamics near the central region of the bilayer. Typical spectra obtained from each probe incorporated into SR in the presence of increasing amounts of melittin are shown in Figure 4. The 5-SASL spectra are more sensitive to the presence of melittin than are the 16-SASL spectra, as evidenced by the 3% decrease in the inner spectral splitting ($2T_\perp'$) and 4% increase in the outer spectral splitting ($2T_\parallel'$) between the control and 10:1 melittin/Ca-ATPase spectra (Table II). As in the case of enzymatic activity, the change in 5-SASL spectral anisotropy is greatest upon the addition of the first

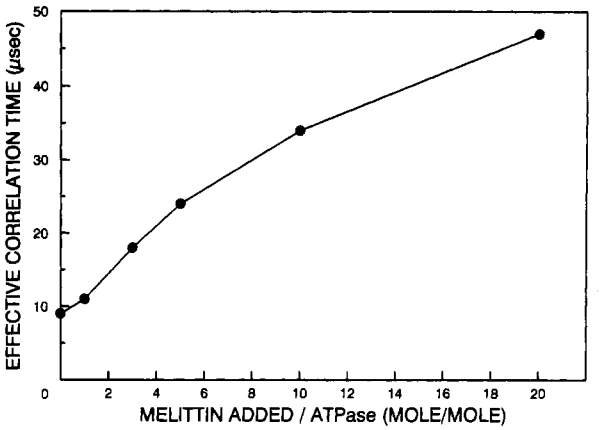

FIGURE 3: Effect of melittin on the effective rotational correlation time (τ_r) of MSL–Ca-ATPase at 25 °C. ST-EPR spectra (Figure 2) were analyzed by using the integrated intensity parameter $\int V_2'$ (Table I), and τ_r was obtained through comparison of this parameter to reference spectra corresponding to isotropic motion (Squier & Thomas, 1986).

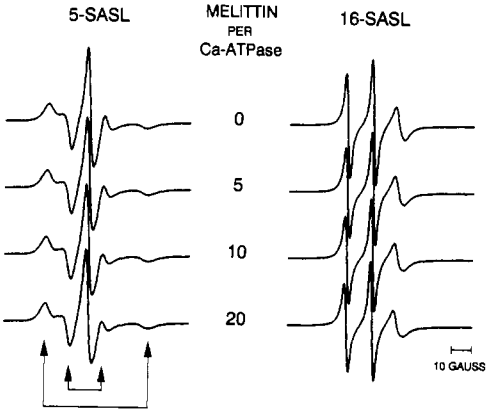

FIGURE 4: Effect of melittin on conventional EPR spectra of probes at different bilayer depths. SR containing either 5- or 16-SASL was incubated with melittin at normal ionic strength for 30 min at 25 °C and prepared for EPR analysis as described under Materials and Methods. Spectra of 5-SASL (left), which report melittin effects near the head-group region of the bilayer, were more sensitive to the presence of increasing melittin than were the spectra of 16-SASL (right), which report melittin effects in the central region of the bilayer. Spectra were characterized by changes in the outer, $2T_\parallel'$, and inner, $2T_\perp'$, spectral splittings (denoted by arrows) with increasing melittin (Table II). Spectra were acquired at 25 °C. Baselines represent 100 G.

Table II: Effect of Melittin on 5- and 16-SASL V_1 EPR Spectral Parameters at 25 °C[a]

	melittin/Ca-ATPase mole ratio				
	control	1:1	3:1	5:1	10:1
5-SASL					
$2T_\parallel'$	53.2 ± 0.3	53.6 ± 0.4	54.3 ± 0.2	54.7 ± 0.3	55.6 ± 0.3
$2T_\perp'$	18.1 ± 0.2	17.9 ± 0.1	17.7 ± 0.1	17.6 ± 0.1	17.6 ± 0.1
Δ_L	3.3 ± 0.1	3.4 ± 0.1	3.4 ± 0.05	3.4 ± 0.05	3.4 ± 0.1
S	0.62 ± 0.01	0.63 ± 0.01	0.65 ± 0.01	0.66 ± 0.01	0.67 ± 0.01
T/η	0.71 ± 0.04	0.58 ± 0.03	0.54 ± 0.02	0.58 ± 0.01	0.54 ± 0.02
16-SASL					
$2T_\parallel'$	32.3 ± 0.1	32.3 ± 0.1	32.0 ± 0.1	32.0 ± 0.2	32.1 ± 0.1
$2T_\perp'$	24.7 ± 0.1	24.8 ± 0.1	24.7 ± 0.1	24.7 ± 0.2	24.6 ± 0.2
Δ_L	1.4 ± 0.1	1.5 ± 0.1	1.6 ± 0.1	1.5 ± 0.1	1.6 ± 0.1
S	0.24 ± 0.01	0.24 ± 0.01	0.24 ± 0.01	0.25 ± 0.01	0.25 ± 0.01
T/η	5.89 ± 0.15	5.88 ± 0.03	5.83 ± 0.11	5.65 ± 0.03	5.54 ± 0.10

[a] Conventional (V_1) EPR parameters: outer splitting, $2T_\parallel'$; inner splitting, $2T_\perp'$; outer half-width at half-height of the low-field peak, Δ_L; order parameter, S; bilayer fluidity, T/η. Parameters $2T_\parallel'$, $2T_\perp'$, and Δ_L, in Gauss, are defined in Figures 2 and 4. Order parameters are calculated from the splitting values by using eqs 1 and 2. Bilayer fluidities (K/centipoise) are calculated from the order parameters by using eq 3. Control corresponds to no-melittin samples, which were treated identically to melittin-containing samples. Errors listed are standard deviations of at least four repetitions.

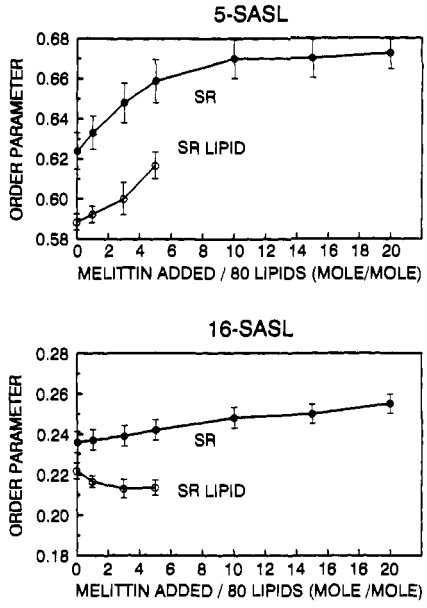

FIGURE 5: Effect of melittin on the order parameter S for 5- (top) and 16- (bottom) SASL incorporated into SR (filled symbols) or protein-free unilamellar vesicles of SR lipids (open circles). Melittin addition is shown per 80 mol of lipid, given the lipid-to-protein ratio of 80:1 in the SR samples (see Materials and Methods). Error bars represent the standard deviation of at least four repetitions.

1–3 mol of melittin per mole of Ca-ATPase, followed by only a small gradual change at higher melittin/Ca-ATPase mole ratios. In contrast, the inner and outer splittings measured from the corresponding 16-SASL spectra are virtually unchanged (<1%) as a function of melittin, which indicates little melittin-induced change in the spectral anisotropy of this label. Slight, but not clearly significant, increases in the linewidth Δ_L, consistent with slower motion or increased heterogeneity, are observed in each set of spectra (Table II).

The observed changes in SASL splittings were quantified in terms of the effective lipid hydrocarbon chain order parameter (eqs 1 and 2, Table II), shown in Figure 5. Progressive binding of melittin to the level of 10:1 melittin/Ca-ATPase increases the order parameter significantly near the head-group region (detected by 5-SASL), but the effects are much less in the central region of the bilayer (detected by 16-SASL). Most of melittin's effects on 5-SASL order occur during the addition of the first 5 mol of melittin per enzyme. These order parameters were used to calculate the effective lipid hydrocarbon chain fluidity (eq 3) at the particular depth of the respective spin label (Table II). Consistent with the melittin-induced increase in SASL order, the binding of 10 melittin per Ca-ATPase decreases the effective fluidity in the head-group region (5-SASL) by 31 ± 8% (from 0.71 ± 0.04 to 0.54 ± 0.02 K/cP) relative to only a 6 ± 4% decrease in the central region (from 5.89 ± 0.15 to 5.54 ± 0.10 K/cP), and further changes at higher melittin levels remain small.

The effect of melittin on SR fluidity is partially reversed by high ionic strength, again strengthening the proposal that the interaction of melittin with SR is characteristic of both hydrophobic and electrostatic forces. As melittin was added to SR in mole ratios of 5:1 and 10:1, the 5-SASL fluidity decreased by only 14% and 17%, respectively, at high ionic strength, compared to the larger decreases (19% and 24%, respectively) at normal ionic strength. The increased ionic strength had no detectable effect on the slight effects of melittin on 16-SASL fluidity.

To test whether melittin's effects on stearic acid spin labels (5-SASL, 16-SASL) arise from a direct electrostatic interaction between melittin's basic residues and the negative charge of the ionized fatty acid carboxyl group, identical experiments were carried out on SR utilizing an uncharged phosphatidylcholine spin label (5-PCSL). In addition to a no-melittin control, 5-PCSL spectra were obtained at melittin levels of 5:1 and 10:1 melittin/Ca-ATPase. At each melittin level, the melittin-induced changes in the spectral splittings (and therefore the effective order parameter and fluidity) are virtually identical (within 0.5%) with those observed for 5-SASL spectra at the same melittin levels. Similarly, high ionic strength reduced the overall effect of melittin on 5-PCSL effective order parameters and fluidities to the same extent (within 1%) as those measured by 5-SASL. These results indicate no direct electrostatic interaction between melittin and the stearic acid labels, increasing confidence that the above SASL results provide a reliable measure of melittin's effects on SR lipids.

Effects of Melittin on Lipid Chain Dynamics in Extracted SR Lipid. To determine the extent to which the Ca-ATPase modulates the melittin–bilayer interaction, similar 5- and 16-SASL spectra were obtained from protein-free unilamellar vesicles composed of extracted SR lipids, and the order parameters obtained from these spectra are shown in Figure 5. The control 5- and 16-SASL spectra of the extracted lipid vesicles displayed slightly narrower $2T_{\parallel}'$ values (5-SASL, 51.7 G; 16-SASL, 32.0 G), and slightly broader $2T_{\perp}'$ (5-SASL, 18.5 G; 16-SASL, 25.0 G) and Δ_L values (5-SASL, 2.4 G; 16-SASL, 1.1 G), indicating smaller effective order parameters (5-SASL, 0.59; 16-SASL, 0.22) relative to the control intact SR vesicles. This is consistent with increased amplitude of probe motion in the protein-free samples, as observed previously in comparisons of SR and SR lipids (Bigelow & Thomas, 1987). For 5-SASL, the increase in effective order parameter with progressive melittin binding was not significantly different from that observed for intact SR (Figure 5). As in the case of intact SR, the effect of melittin on SR lipid was smaller for 16-SASL than for 5-SASL. However, the order parameter actually decreased slightly for 16-SASL in SR lipid. Conversion of each order parameter to the effective lipid hydrocarbon chain fluidity (eq 3) shows the same trends: that is, the protein-free bilayers are more fluid (i.e., 5-SASL control, 0.856 K/cP; 16-SASL control, 6.39 K/cP) than SR membranes, and melittin affects the head-group region more (0.733 K/cP at 5 melittin per 80 lipids, a 16% decrease) than the central region (6.68 K/cP at 5 melittin per 80 lipids, a 4% increase). We performed similar studies on multilamellar lipid dispersions (data not shown) prepared as described previously (Bigelow et al., 1986). Melittin had virtually no effect on EPR spectra of 5- or 16-SASL in these dispersions, probably because melittin cannot cross lipid bilayers, and thus only contacts the outer bilayer in each multilamellar vesicle, while stearic acid spin labels distribute themselves uniformly throughout the multilamellae.

Discussion

Summary. We have used conventional EPR and ST-EPR to analyze the effects of melittin on the rotational dynamics of the SR Ca-ATPase and lipids. The results, summarized in Figure 6, indicate that melittin substantially inhibits Ca-ATPase activity and rotational mobility while only slightly inhibiting lipid hydrocarbon chain rotation. These results are consistent with previous studies in this laboratory, supporting the proposal that Ca-ATPase rotational mobility and SR lipid fluidity are essential for optimal calcium uptake. On a more general level, the interactions of amphipathic peptides and other surface-binding proteins with membranes are of great

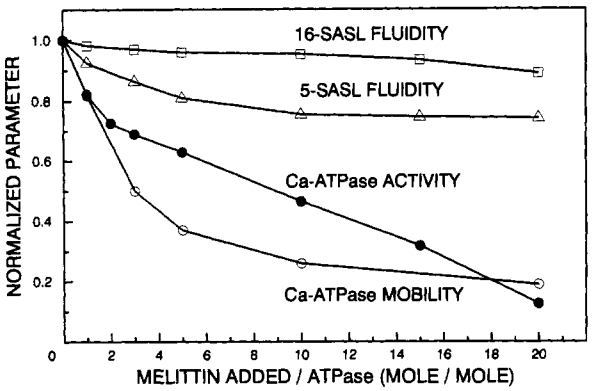

FIGURE 6: Relationship of the effect of melittin on ATPase activity, Ca-ATPase rotational mobility, and SR lipid fluidity at 25 °C. Values of Ca-ATPase activity (Figure 2), protein mobility (τ_r^{-1} from Table I), and lipid fluidity (empirical quantity calculated from apparent order parameters) from 5- and 16-SASL spectra (Table II) are compared by normalizing each parameter to its respective no-melittin control value. Each point represents the average of at least three repetitions. Standard deviations of lipid data were comparable to the size of the data points, and standard deviations of activity and mobility data were less than 10%.

interest, and a physical understanding of these interactions requires the direct detection of effects on both lipids and integral membrane proteins. While a number of studies have investigated the physical interaction of surface-binding proteins with lipid bilayers, the present study extends this field to include (1) an intact biological membrane, (2) physical effects on both lipids and integral proteins, and (3) effects on biological function.

Melittin Inhibits Ca-ATPase Rotational Mobility Substantially. Previous studies in this laboratory have demonstrated a relationship between Ca-ATPase enzymatic activity and rotational mobility (Squier & Thomas, 1988; Squier et al., 1988a; Birmachu & Thomas, 1990). Finding that melittin inhibits both ATPase activity and Ca-ATPase mobility is consistent with such a relationship. Like the effect of melittin on enzymatic activity, the effect on protein mobility is biphasic. The decrease in protein mobility correlates particularly well with the loss of ATPase activity during the binding of the first 1–5 mol of melittin per Ca-ATPase, where the initial slopes of melittin-induced inhibition of Ca-ATPase activity and mobility are nearly identical (Figure 6). Further, the effect of melittin on enzyme mobility is only partially decreased by increased ionic strength, suggesting components of inhibition that arise from both hydrophobic and electrostatic interactions between melittin and SR.

From the hydrodynamic theory of Saffman and Delbrück (1975; eq 4 in the present study), the progressive decrease of Ca-ATPase mobility with increasing melittin could be due either to (a) a decrease in the rate ($1/\tau_r$) of rotation of a single rotating species, due to an increase in membrane viscosity (η in eq 4), i.e., a decrease in fluidity, or (b) an increase in the average cross-sectional area of the rotating units in the plane of the membrane (πa^2 in eq 4), due to an increase in protein association (aggregation). Since ST-EPR is a steady-state spectroscopic technique, it does not provide time-resolved information about the populations and rates of individual rotating units (i.e., monomer/dimer vs large aggregate rotation). Therefore, lipid data are needed to determine whether melittin's effects are primarily on lipid fluidity or protein aggregation.

Melittin Restricts Lipid Chain Dynamics Slightly. Previous studies in this laboratory and others have demonstrated a relationship between SR membrane fluidity and Ca-ATPase activity [reviewed by Thomas (1986) and Hidalgo (1985)], primarily since membrane fluidity controls Ca-ATPase rotational mobility (Squier et al., 1988b). Hydrodynamic theory predicts that the rotational diffusion coefficient (proportional to mobility) of an integral protein about the membrane normal should be proportional to the fluidity (inverse viscosity, eq 4) of the surrounding lipid bilayer (Saffman & Debrück, 1975), and previous EPR studies have confirmed this relationship in SR (Hidalgo et al., 1978; Bigelow & Thomas, 1987; Squier et al., 1988b; Birmachu & Thomas, 1990). The melittin-induced decrease in SR lipid hydrocarbon chain fluidity, as probed by 5-SASL, correlates with decreasing enzyme mobility and activity, especially during the binding of the first 5 mol of melittin per Ca-ATPase (Figure 6), suggesting that melittin's inhibition of Ca-ATPase rotational mobility and activity arises from melittin's restriction of lipid chain dynamics. However, while the change in fluidity is in the right direction (a decrease) to slow protein rotation, the total decrease in fluidity is much smaller than the decreases of enzyme mobility and activity. Hydrodynamic theory (Saffman & Delbrück, 1975) predicts that integral protein rotational mobility is directly proportional to lipid fluidity (inverse viscosity, eqs 3 and 4), so *only a small part of the reduced protein mobility can be attributed to reduced lipid fluidity. Therefore, most of the reduction in protein mobility must be due to an increase in the cross-sectional area of the rotating unit in the plane of the membrane (πa^2 in eq 4), i.e., to lateral aggregation of the enzyme.*

Melittin Interacts Primarily Near the Membrane Surface. The orientation of melittin when bound to model bilayers has been considered in a number of studies [reviewed by Dempsey (1990)], with inconclusive results. Our results with an intact membrane demonstrate clearly that melittin's perturbation of lipid fluidity is depth dependent (Figure 6) such that the perturbation is greatest near the head-group region of the bilayer, leaving the center of the bilayer nearly unaffected. This indicates that melittin lies predominantly on the membrane surface (parallel to the plane of the membrane), consistent with several previous studies on model lipid vesicles (Maurer et al., 1991; Batenburg et al., 1987; Schulze et al., 1987; Altenbach & Hubbell, 1988; Altenbach et al., 1989). Therefore, any lipid-mediated reduction of Ca-ATPase rotational mobility and activity is due primarily to melittin perturbations near the bilayer surface. Experiments using protein-free SR lipid vesicles support this conclusion. Melittin decreases the fluidity of the head-group region of these lipid vesicles to the same extent as in intact SR, whereas a slight increase in fluidity is observed in the center of the lipid bilayer (Figure 5A).

Stearic acid spin labels are known to position themselves such that the α-carbon of the fatty acid chain is aligned with the head-group region of the bilayer. As a result, these probes are expected to report reliably the degree of orientational order and dynamics of the host lipid molecules at a depth determined by the position of the nitroxide on the hydrocarbon chain (Marsh, 1981; Squier & Thomas, 1989). Nevertheless, two possible problems with these probes must be addressed in the present study. First, nitroxides on stearic acid probes undergo vertical fluctuations relative to the membrane normal, such that the label is located over a distribution of vertical locations (Davoust et al., 1983; Feix et al., 1984, 1987; Ellena et al., 1988). However, this fluctuation does not prevent nitroxides at different positions along the hydrocarbon chain from providing depth-dependent information, especially if (a) nitroxides positioned near the carboxyl terminus and the methyl chain

terminus are compared and (b) the stearic acid spin labels are incorporated into bilayers possessing some degree of unsaturation (Feix et al., 1984, 1987). In the present study, stearic acid spin probes with nitroxides at the C-5 and C-16 hydrocarbon positions are utilized with confidence, knowing that the SR membrane contains a high degree of unsaturated lipid hydrocarbon chains (Hidalgo, 1985). Second, since stearic acid spin labels under conditions similar to those of the present study have been shown to be nearly fully ionized at pH 7.0 (Squier et al., 1991), the negatively charged labels could participate in direct electrostatic interactions with the basic residues of membrane-bound melittin. However, experiments utilizing a nonionizable phosphatidylcholine spin label, 5-PCSL, gave results virtually identical with those obtained from the analogous stearic acid spin label, suggesting that any direct melittin–label interaction is negligible. This is supported by the observation that the SASL spectra show no evidence of a new melittin-induced spectral component, which could be interpreted in terms of a melittin–SASL complex. Therefore, under the conditions of the present study, the stearic acid spin labels should faithfully report bilayer lipid order and dynamics at their respective depths (Feix, et al., 1987) while providing discrete information about the bilayer fluidity gradient from the head-group region to the central region of the bilayer (Marsh, 1981; Squier & Thomas, 1989).

Correlation with Ca-ATPase Activity. Melittin inhibits Ca-ATPase enzymatic activity in a biphasic manner (Figure 5). The initial component of inactivation (1–3 mol of melittin per Ca-ATPase) is unaffected by an increase in the ionic strength of the medium (Voss et al., 1991), suggesting that a hydrophobic interaction between melittin and the membrane is responsible for this inhibition. This interpretation is supported by the 5-SASL fluidity results, which show a similar initial decrease. The more gradual component of inactivation is completely reversed by increasing ionic strength (Voss et al., 1991), suggesting a weaker electrostatic interaction between melittin and SR. The ST-EPR results are also biphasic, suggesting that both phases of enzyme inactivation correspond to ATPase aggregation of melittin, consistent with previous studies showing that enforced interactions among Ca-ATPase molecules inhibit enzymatic activity (Squier & Thomas, 1988; Squier et al., 1988a; Birmachu & Thomas, 1990; Voss et al., 1991). Partial reversal of melittin's effects by increased ionic strength supports the suggestion that melittin interacts with SR both by hydrophobic and electrostatic forces. The particular mechanistic step(s) perturbed by melittin remains a subject for future study. Hidalgo et al. (1978) and Squier and Thomas (1988) proposed that Ca-ATPase mobility facilitates the enzymatic step(s) involving phosphoenzyme decomposition. A detailed kinetic study, asking whether melittin binding to SR perturbs enzyme phosphorylation or dephosphorylation, would test this proposal further while providing insight into the mechanism of melittin-induced Ca-ATPase inhibition.

Relationship to Complementary Optical Spectroscopy Measurements. Investigators in this laboratory have also studied the effects of melittin on the rotational dynamics of the SR Ca-ATPase and lipids as measured by time-resolved phosphorescence anisotropy (TPA) and fluorescence anisotropy (TFA), respectively (Voss et al., 1991). As in the present EPR study, the optical results show that melittin strongly inhibits protein rotational mobility, while having only a small effect on lipid order. Neither effect can be fully reversed by increased ionic strength.

The TPA results of Voss et al. (1991) provide information that complements the ST-EPR study. The time-resolution of TPA showed clearly that melittin's primary effect is to induce protein aggregation, supporting this interpretation of the ST-EPR data. A small but significant difference between the ST-EPR results and TPA study (Voss et al., 1991) is that the TPA results show that Ca-ATPase mobility continues to decrease at high melittin levels whereas the ST-EPR results show that the inhibition of mobility appears to saturate above 10 mol of melittin per Ca-ATPase (Figure 6). It is possible that the apparent saturation of melittin's effects on protein mobility detected by ST-EPR may be artifactual; that is, the overall rotation of the aggregated ATPase may become slower than the inherent segmental motion of the spin label itself relative to the protein backbone, resulting in ST-EPR spectra that are increasingly dominated by the constant motion of the spin label in its microenvironment rather than the slowing motion of the aggregating ATPase (Lewis & Thomas, 1986; Horvâth, et al., 1990; Squier & Thomas, 1986a; Thomas, 1986). This ambiguity is resolved by TPA, since the motions of the label, protein, and large aggregates are resolved in time and analyzed independently. Still, the ST-EPR study is advantageous in that the Ca-ATPase incorporates maleimide spin label with very little loss of activity, a result not found with the erythrosin-5-isothiocyanate label used in the TPA study.

The EPR results concerning melittin–lipid interactions in the present study extend significantly the TFA study, in which diphenylhexatriene (DPH) has been used to probe lipid chain dynamics (Voss et al., 1991). Compared with DPH, stearic acid spin labels provide more detailed information on the depth-dependence of melittin-induced changes in orientational order and dynamics of lipid molecules in the membrane. Spin labels also provide a more reliable measurement of lipid fluidity, which has been calibrated empirically (Squier et al., 1988b), so EPR provides a more quantitative assessment of the extent to which changes in membrane fluidity affect Ca-ATPase mobility and activity. Experiments on extracted SR lipids, performed in the present EPR study but not in the TFA study (Voss et al., 1991), clarify the role of the Ca-ATPase in melittin–lipid interactions.

A Model for Melittin–SR Interaction. The above results suggest that melittin inhibits the Ca-ATPase primarily by binding to the membrane surface and inducing lateral aggregation of the Ca-ATPase molecules. Previous studies by Cherry and co-workers have shown that the amphipathic nature of melittin is the key aspect of its action against membranes and membrane proteins. A direct comparison between melittin and polylysine has shown that melittin's hydrophobic nature is essential for its ability to interact with membrane proteins (Clague & Cherry, 1989), while melittin charge neutralization studies (Dufton et al., 1984) have demonstrated that it is the highly basic nature of the peptide's C-terminus which is responsible for its ability to aggregate band 3 of erythrocyte membranes. Clague and Cherry (1989) proposed a model describing melittin-induced membrane protein aggregation in which the hydrophobic portion of melittin partitions into the bilayer, thereby anchoring the basic moieties close to the membrane surface. The basic groups on the peptide are then positioned properly to neutralize the repulsion from negative charges on the membrane surface, between phospholipid head-groups and integral proteins and/or between integral proteins themselves. Clearly, the results of the present study agree with this model: (1) melittin's gradient effect in decreasing the lipid chain dynamics of the bilayer is consistent with a predominantly surface-bound (anchored) peptide and (2) melittin-induced inhibition of Ca-ATPase mobility is consistent with the peptide's ability to aggregate ATPase

polypeptides. Such a model, which depends heavily on both the hydrophobic (membrane associating) and hydrophilic (protein associating) properties of melittin, suggests that the peptide might interact at the boundary between protein and lipid; future studies should focus on whether melittin changes the number and/or dynamics of Ca-ATPase boundary lipids. In relating melittin-induced changes in the physical properties of membrane fluidity and protein mobility with changes in enzyme activity, the present study provides an important extension of this model: the results should provide new insight into the membrane-perturbing mechanism of action of surface-active peptides in regulating the physical state and biological function of integral membrane proteins. Specific examples include phospholamban [known to regulate the cardiac Ca-ATPase (Tada & Katz, 1982; James et al., 1989)], signal sequences such as presequence p25 [known to promote translocation of cytochrome oxidase subunit IV across the mitochondrial membrane (Clague & Cherry, 1988)], and mast-cell-triggering peptides [known to promote secretion of inflammation mediators from mast cells (Dufton et al., 1984)]. This study and that of Voss et al. (1991), combined with further characterization of the melittin–SR interaction, should provide a better understanding of the mechanism of action of these and similar peptides in membrane systems.

Conclusions. Melittin binding to SR results in substantial inhibition of Ca-ATPase activity, which correlates with melittin-induced inhibition of enzyme mobility and a restriction of lipid chain dynamics. Our results argue that (1) melittin affects enzyme activity primarily by aggregating the enzyme, most likely by interacting directly with the Ca-ATPase and (2) this process occurs, at least in part, at the membrane surface since melittin perturbs lipid hydrocarbon chain mobility predominantly at the surface. The results provide insight into the mechanism of action of melittin, and amphipathic membrane-binding peptides in general, by showing how such peptides interact with membrane proteins and lipids. The results also provide further evidence that the rotational dynamics of lipid and the Ca-ATPase in SR are important for optimal calcium uptake. Future studies should be directed toward better characterizing the physical interaction between melittin and SR while providing more detailed insight into the kinetic nature of enzyme inhibition by melittin.

Acknowledgments

We thank John Voss for providing purified melittin and unpublished data on melittin's interaction with SR. We are grateful to Brad Karon, Debbie Hussey, and Razvan Cornea for their assistance with various phases of this work, Gary Nelsestuen for the use of the vesicle extrusion device, Erik Rivers and Dean Binger for their technical assistance in SR preparation and related assays, Bob Bennett for developing our EPR analysis software and handling spectrometer trouble-shooting and repair, Franz Nisswandt for building and customizing our computer network and file server, and Woubalem Birmachu and Derek Marsh for many helpful discussions concerning this study.

References

Altenbach, C., & Hubbell, W. L. (1988) *Proteins: Struct., Funct., Genet. 3*, 230–242.

Altenbach, C., Froncisz, W., Hyde, J. S., & Hubbell, W. L. (1989) *Biophys. J. 56*, 1183–1191.

Batenburg, A. M., Hibbeln, J. C. L., & de Kruijff, B. (1987) *Biochim. Biophys. Acta 903*, 155–165.

Benga, G., & Holmes, R. P. (1984) *Prog. Biophys. Mol. Biol. 43*, 195–252.

Beschiaschvili, G., & Seelig, J. (1990) *Biochemistry 29*, 52–58.

Bigelow, D. J., & Thomas, D. D. (1987) *J. Biol. Chem. 262*, 13449–13456.

Bigelow, D. J., Squier, T. C., & Thomas, D. D. (1986) *Biochemistry 25*, 194–202.

Birmachu, W., & Thomas, D. D. (1990) *Biochemistry 29*, 3904–3914.

Birmachu, W., Nisswandt, F. L., & Thomas, D. D. (1989) *Biochemistry 28*, 3940–3947.

Bradrick, T. B., Dasseux, J., Abdalla, M., Aminzadeh, A., & Georghiou, S. (1987) *Biochim. Biophys. Acta 900*, 17–26.

Bradrick, T. D., Freire, E., & Georghiou, S. (1989) *Biochim. Biophys. Acta 982*, 94–102.

Chen, P. S., Toribara, T. Y., & Warner, H. (1956) *Anal. Chem. 28*, 1756–1758.

Clague, M. J., & Cherry, R. J. (1988) *Biochem. J. 252*, 791–794.

Clague, M. J., & Cherry, R. J. (1989) *Biochim. Biophys. Acta 980*, 93–99.

Cuppoletti, J. (1990) *Arch. Biochem. Biophys. 278*, 409–415.

Davoust, J., Seigneuret, M., Herve, P., & Devaux, P. F. (1983) *Biochemistry 22*, 3146–3151.

Dempsey, C. E. (1990) *Biochim. Biophys. Acta 1031*, 143–161.

Dempsey, C. E., & Sternberg, B. (1991) *Biochim. Biophys. Acta 1061*, 175–184.

Dempsey, C., Bitbol, M., & Watts, A. (1989) *Biochemistry 28*, 6590–6596.

Dufourc, E. J., Smith, I. C. P., & Dufourcq, J. (1986) *Biochemistry 25*, 6448–6455.

Dufton, M. J., Hider, R. C., & Cherry, R. J. (1984a) *Eur. Biophys. J. 11*, 17–24.

Dufton, M. J., Cherry, R. J., Coleman, J. W., & Stanworth, D. R. (1984b) *Biochem. J. 223*, 67–71.

Ellena, J. F., Archer, S. J., Dominey, R. N., Hill, B. D., & Cafiso, D. S. (1988) *Biochim. Biophys. Acta 940*, 63–70.

Faucon, J. F., & Lakowicz, J. R. (1987) *Arch. Biochem. Biophys. 252*, 245–258.

Feix, J. B., Popp, C. A., Venkataramu, S. D., Beth, A. H., Park, J. H., & Hyde, J. S. (1984) *Biochemistry 23*, 2293–2299.

Feix, J. B., Yin, J.-J., & Hyde, J. S. (1987) *Biochemistry 26*, 3850–3855.

Fernandez, J. L., Rosemblatt, M., & Hidalgo, C. (1980) *Biochim. Biophys. Acta 599*, 552–568.

Folch, J., Lees, M., & Sloane-Stanley, G. H. (1957) *J. Biol. Chem. 226*, 497–509.

Gaffney, B. J. (1976) in *Spin Labeling Theory and Practice* (Berliner, L. J., Ed.) pp 567–571, Academic Press, New York.

Gornall, A. G., Bardawill, C. J., & David, M. M. (1949) *J. Biol. Chem. 177*, 751–766.

Hidalgo, C. (1985) in *Membrane Fluidity in Biology* (Boggs, J. M., & Aloia, R. C., Eds.) Vol. 4, pp 51–96, Academic Press, New York.

Hidalgo, C., Ikemoto, N., & Gergely, J. (1976) *J. Biol. Chem. 251*, 4224–4232.

Hidalgo, C., Thomas, D. D., & Ikemoto, I. (1978) *J. Biol. Chem. 253*, 6879–6887.

Horvâth, L. I., Dux, L., Hankovszky, H. O., Hideg, K., & Marsh, D. (1990) *Biophys. J. 58*, 231–241.

Hu, K.-S., Dufton, M. J., Morrison, I., & Cherry, R. J. (1985) *Biochem. Biophys. Acta 816*, 358–364.

Hui, S. W., Stewart, C. M., & Cherry, R. J. (1990) *Biochim. Biophys. Acta 1023*, 335–340.

James, P., Inui, M., Tada, M., Chiesi, M., & Carafoli, E. (1989) *Nature 342*, 90–92.
Kataoka, M., Head, J. F., Seaton, B. A., & Engelman, D. M. (1989) *Proc. Natl. Acad. Sci. U.S.A. 86*, 6944–6948.
Kuchinka, E., & Seelig, J. (1989) *Biochemistry 28*, 4216–4221.
Lafleur, M., Faucon, J.-F., Dufourcq, J., & Pézolet, M. (1989) *Biochim. Biophys. Acta 980*, 85–92.
Laggner, P., & Barratt, M. D. (1975) *Arch. Biochem. Biophys. 170*, 92–101.
Lewis, S. M., & Thomas, D. D. (1986) *Biochemistry 25*, 4615–4621.
Malencik, D. A., & Anderson, S. R. (1985) *Biochem. Biophys. Res. Commun. 130*, 22–29.
Malencik, D. A., & Anderson, S. R. (1988) *Bicohemistry 27*, 1941–1949.
Marsh, D. (1981) in *Membrane Spectroscopy* (Grell, E., Ed.) Vol. 31, pp 51–142, Springer-Verlag, Berlin.
Maurer, T., Lücke, C., & Rüterjans, H. (1991) *Eur. J. Biochem. 196*, 135–141.
O'Brian, C. A., & Ward, N. E. (1989) *Mol. Pharmacol. 36*, 355–359.
Popp, C. A., & Hyde, J. S. (1981) *J. Magn. Reson. 43*, 249–258.
Prendergast, F. G., Lu, J., Wei, G. J., & Bloomfield, V. A. (1982) *Biochemistry 21*, 6963–6970.
Raynor, R. L., Zheng, B., & Kuo, J. F. (1991) *J. Biol. Chem. 266*, 2753–2758.
Saffman, P. J., & Delbrück, M. (1975) *Proc. Natl. Acad. Sci. U.S.A. 72*, 3111–3113.
Schulze, J., Mischeck, U., Wigand, S., & Galla, H.-J. (1987) *Biochim. Biophys. Acta 901*, 101–111.
Schwarz, G., & Beschiaschvili, G. (1989) *Biochim. Biophys. Acta 979*, 82–90.
Shinitzky, M. (1984) in *Physiology of Membrane Fluidity* (Shinitzky, M., Ed.) Vol. 1, pp 1–51, CRC Press, Inc., Boca Raton, FL.
Squier, T. C., & Thomas, D. D. (1986a) *Biophys. J. 49*, 921–935.
Squier, T. C., & Thomas, D. D. (1986b) *Biophys. J. 49*, 937–942.
Squier, T. C., & Thomas, D. D. (1988) *J. Biol. Chem. 263*, 9171–9177.
Squier, T. C., & Thomas, D. D. (1989) *Biophys. J. 56*, 735–748.
Squier, T. C., Hughes, S. E., & Thomas, D. D. (1988a) *J. Biol. Chem. 263*, 9162–9170.
Squier, T. C., Bigelow, D. J., & Thomas, D. D. (1988b) *J. Biol. Chem. 263*, 9178–9186.
Squier, T. C., Lakowicz, J. R., Mahaney, J. E., Yin, J.-J., and Lai, C.-S. (1991) *Biophys. J. 59*, 654–669.
Tada, M., & Katz, A. M. (1982) *Annu. Rev. Physiol. 44*, 401–423.
Thomas, D. D. (1986) in *Techniques for the Analysis of Membrane Proteins* (Ragan, C. I., & Cherry, R. J., Eds.) pp 377–431, Chapman and Hall, London.
Voss, J., Birmachu, W., Hussey, D., & Thomas, D. D. (1991) *Biochemistry* (in press).
Wille, B. (1989) *Anal. Biochem. 178*, 118–120.
Yeagle, P. L. (1985) *Biochim. Biophys. Acta 822*, 267–287.

Amino Acid Sequence of Nitrite Reductase: A Copper Protein from *Achromobacter cycloclastes*†

Faith F. Fenderson,‡ Santosh Kumar,§ Elinor T. Adman,*,‡ M.-Y. Liu,∥ W. J. Payne,⊥ and Jean LeGall∥
Departments of Biological Structure and Biochemistry, University of Washington, Seattle, Washington 98195, and Departments of Biochemistry and Microbiology, University of Georgia, Athens, Georgia 30406
Received January 23, 1991; Revised Manuscript Received March 13, 1991

ABSTRACT: The amino acid sequence of the copper-containing nitrite reductase (EC 1.7.99.3) from *Achromobacter cycloclastes* strain IAM 1013 has been determined by using peptides derived from digestion with *Achromobacter* protease I (Lys), *Staphylococcus aureus* V8 protease (Glu), cyanogen bromide, and BNPS-skatole in acetic acid. The subunit contains 340 amino acids. The identity of the first seven amino acids is tentative. The sequence has been instrumental in the X-ray structure determination of this molecule; in conjunction with the X-ray structure, ligands to a type I copper atom and a type II copper atom (one of each per subunit) have been identified. Comparison of the sequence to those of multi-copper oxidases such as ascorbate oxidase, laccase, and ceruloplasmin [Messerschmidt, A., & Huber, R. (1990) *Eur. J. Biochem. 187*, 341–352] reveals that each of two domains seen in the X-ray structure is similar to the oxidases and also to the small blue copper-containing proteins such as plastocyanin. The *combination* of sequence and structural similarity to ascorbate oxidase and sequence similarity to ceruloplasmin leads to a plausible model for the domain structure of ceruloplasmin.

Nitrite reductase (NIR) catalyzes the reduction of nitrite as part of the dissimilatory pathway in which dentrifying bacteria convert nitrate to nitrogen (Payne, 1985):

$$NO_3^- \rightarrow NO_2^- \rightarrow NO \rightarrow N_2O \rightarrow N_2$$

The reaction product of NIR in vivo has been shown to be nitric oxide (NO) (Liu et al., 1986; Iwasaki & Matsubara, 1972). The reduction of nitrite to nitric oxide and the reduction of nitric oxide to nitrous oxide are two independent reactions in *Achromobacter cycloclastes* (Shapleigh & Payne,

† This work was supported by NIH Grants GM31770 and GM15731 and by NSF Grant DMB-8718646.
* Author to whom correspondence should be addressed.
‡ Department of Biological Structure, University of Washington.
§ Department of Biochemistry, University of Washington.
∥ Department of Biochemistry, University Georgia.
⊥ Department of Microbiology, University Georgia.

0006-2960/91/0430-7180$02.50/0